IMWA 2026
Jeongseon

Global Copper Supply Under Climate-Driven Water Stress: A Proof of Concept

Mariam Taki[1], Nicolas Flipo[2], Damien Goetz[3]

[1]*Department of Geosciences, Paris School of Mines, PSL University, France, mariam.taki@minesparis.psl.eu, ORCID 0009-0007-3864-1611*

[2]*Department of Geosciences, Paris School of Mines, PSL University, France, nicolas.flipo@minesparis.psl.eu, ORCID 0000-0002-8099-2104*

[3]*Department of Geosciences, Paris School of Mines, PSL University, France, damien.goetz@minesparis.psl.eu, ORCID 0009-0007-4740-4255*

Abstract

A global framework assessing climate-driven hydrology for mineral production was applied to evaluate water availability for porphyry copper production. Using validated historical simulations and SSP2-4.5 projections, extractable water from rivers, lakes, and aquifers was quantified, and monthly mining water stress was calculated under a grade-based production schedule. Results identified temporal and spatial hotspots where water demand approached or exceeded local availability, with peak stress exceeding 100% in northern Chile. The framework demonstrated the feasibility of linking climate-driven hydrology to mineral-specific production and highlighted the importance of integrating water resources into mine planning under changing climatic conditions.

Keywords: Water stress, climate change, copper, hydrology, mine water management

Introduction

Water availability constrains mining operations through its role in mineral extraction, processing, dust suppression, and tailings management (Gunson *et al.* 2012). For large-scale metal production, sustained access to water is required over multi-decadal timescales, making mining systems sensitive to long-term changes in hydrological conditions. Climate change alters precipitation patterns, evapotranspiration, runoff generation, groundwater recharge, and surface water storage, directly affecting the volume and timing of water that can be physically extracted for industrial use.

Copper is central to electrification and energy system transitions, and porphyry deposits account for the majority of global copper supply. Assessing whether climate-driven changes in water availability may constrain copper extraction therefore represents a relevant problem for mine water management and long-term supply planning.

Existing assessments of mining water risk often rely on static water stress indicators that do not reflect climate-driven variability or low-flow conditions relevant to mine operations (Lakshman 2024) (Northey 2017). At the global scale, few approaches combine physically based hydrology, historical validation against observations, and mineral-specific water demand in a single framework. This limits the ability to identify when and where water availability may act as a binding constraint on production under evolving climatic conditions.

Climate-driven changes in water availability were evaluated at the global scale using HyIR, a hydrological aggregation framework developed to translate climate projections into physically based estimates of extractable water. Outputs from the hydrological framework were then combined with a process-based model of water demand for porphyry copper extraction to assess mining water stress. This application provided a proof of concept for linking climate-informed water availability with mineral-specific production requirements.

Methods

Climate-driven water availability was assessed using the HYdrological and Industrial Resilience (HyIR) framework, a global-scale hydrological aggregator developed to translate outputs from the Coupled Model Inter-comparison Project Phase 6 (CMIP6) general circulation models into physically interpretable indicators of extractable water (Eyring *et al.* 2016). The framework was forced with outputs from the first Taiwanese Earth System Model TaiESM1 for the historical period and under the Shared Socioeconomic Pathway SSP2-4.5, reflecting moderate greenhouse gas emissions scenario also referred to as "Middle of the road" scenario, and was applied at the native spatial resolution of the climate model (1.25° × 0.9°) with monthly time steps (Lee *et al.* 2020).

HyIR represents water evolution through three coupled components: storage in lakes and reservoirs, groundwater storage in aquifer systems, and river discharge including explicit routing (Fig. 1). The framework produces gridded time series of gross extractable water, defined as the volume of water that could be withdrawn from each component while remaining physically sustainable, without accounting for infrastructure constraints, sectoral allocation, or water rights. Reservoir and lake availability was based on a fixed fraction of stored volume ensuring a minimum persistence of 10 years without recharge, river availability on flows exceeding a 30-day low-flow threshold defined from long-term quantiles, and groundwater availability on accessible aquifer storage limited by permeability and a 50-year depletion constraint. Indicators evolved dynamically in response to climate forcing and were aggregated at the climate model grid scale.

To better represent basin-scale hydrology and improve agreement with observed river discharge, three correction factors were introduced and calibrated: a redistribution factor controlling the fraction of infiltration redirected to surface runoff, a seasonal baseflow multiplier adjusting groundwater contribution through the year, and a time-of-concentration multiplier affecting river discharge routing. These corrections were evaluated against observed discharge from the Global Runoff Data Centre (GRDC 2026) using a modified drought-focused Kling-Gupta Efficiency metric KGE-d (Schaefli and Gupta 2007). The metric ranges from $-\infty$ to 1, where 1 indicates perfect agreement between simulated and observed discharge, and is defined as:

$$KGE_d = 1 - \sqrt{(r-1)^2 + (\beta-1)^2 + (\gamma-1)^2}$$

where r is the linear correlation coefficient, β is the ratio of simulated to observed mean discharge, and γ is the ratio of QMNA5 low-flow quantiles. QMNA5 represents the minimum 30-day mean discharge with a 5-year return period, used here to characterize low-flow conditions. Following Knoben *et al.* (2019), a value of –0.41 was adopted as the threshold for acceptable performance, corresponding to the score obtained when simulated discharge is equal to the observed mean value, meaning that values above this threshold perform better than a mean-flow benchmark. Validation was performed over the historical period 1850–2015 using observed and simulated daily discharge for large river basins with available data.

Water demand for porphyry copper production was estimated using a process-based, bottom-up model representing on-site mining and mineral processing operations up to the production of copper concentrate. The model accounted for water inputs, internal recycling, and losses primarily associated with tailings management and evaporation (Fig. 2). Copper production was represented using a publicly available global database of porphyry copper deposits (Magnin *et al.* 2025), with water demand computed using deposit-specific parameters, empirically derived production scheduling rules, processing configurations, and a conceptual representation of tailings-related water flows.

Copper production was scheduled to meet demand trajectories from the International Energy Agency Stated Policies Scenario STEPS, reflecting a moderate energy transition scenario consistent with the SSP2-4.5 climate pathway, over the period 2025-2050 (IEA 2024). Scheduling followed a descending ore-grade order and

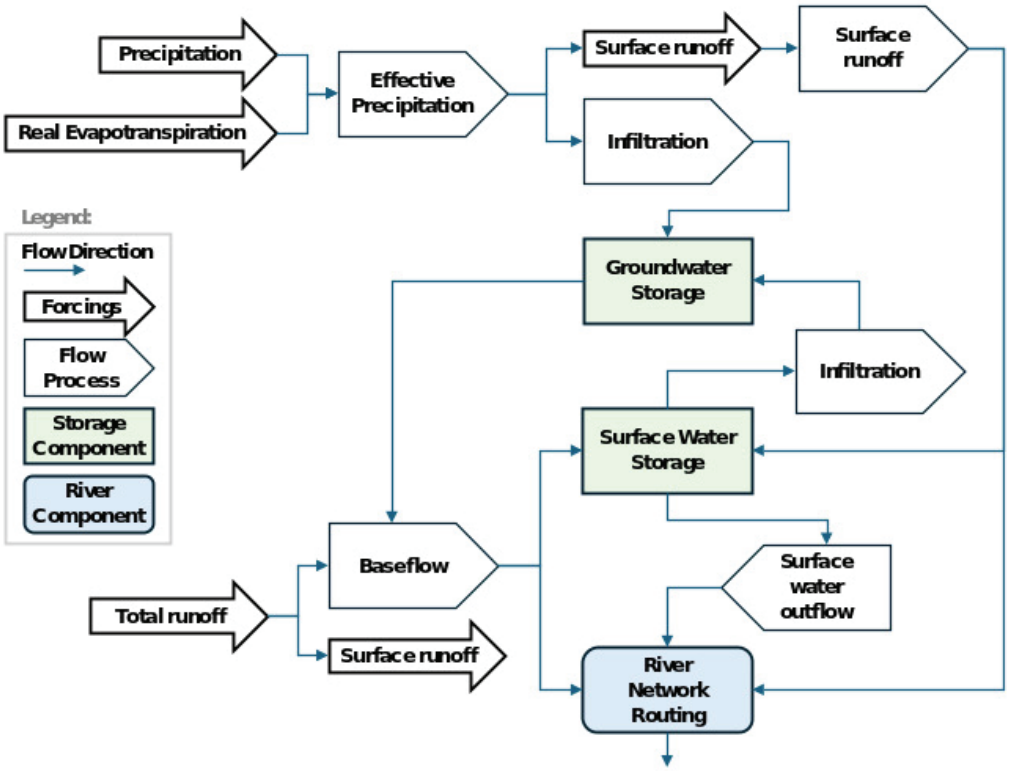

Figure 1 Schematic overview of HyIR.

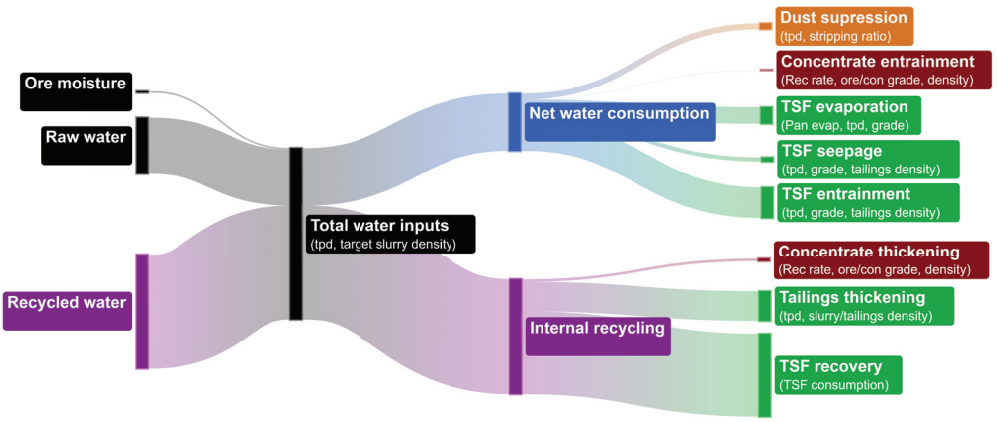

Figure 2 Water flows considered in the model.

was scaled to represent global copper supply by scaling demand to porphyry deposits, assumed to continuously account for 82% of identified copper resources. New deposits were activated as existing operations were exhausted to reduce the demand–supply gap.

Monthly mining water stress was quantified as the ratio of monthly water demand associated with scheduled copper production, aggregated spatially to the hydrological grid, to a fixed fraction of monthly gross extractable water allocated for mining

within the corresponding grid cell. Where extractable water availability approaches zero, the ratio loses interpretability, such cases were therefore flagged.

Results

Simulated river discharge from HyIR, forced with historical TaiESM1 data, was compared to GRDC observations across South America for the period 1850–2015 (Fig. 3a). Observations were available for large basins covering 71.6% of the continent. Using the −0.41 performance threshold, 69.9% of the assessed area exhibited KGE-d values above the benchmark, indicating that HyIR simulations forced with historical TaiESM1 data reproduced hydrological variability more effectively than assuming stationary mean flows. Lower scores representing 30.1% of the assessed area were mainly observed in relatively small coastal basins characterized by extreme precipitation (>2600 mm a^{-1}), where forcing precipitation exceeded observed discharge by more than 1000%, indicating unrealistically wet forcing conditions in TaiESM1 rather than structural limitations of the HyIR framework.

Using the validated HyIR configuration, extractable water availability was simulated from TaiESM1 projections under the SSP2-4.5 moderate scenario. Monthly extractable water was computed at the climate model grid scale as the aggregate contribution from lakes and reservoirs, river discharge, and groundwater storage (Fig. 3b). The resulting fields represented physically based estimates of gross extractable water availability derived from climate forcing and hydrological storage dynamics and formed the hydrological input for subsequent mining water stress calculations.

Scheduled copper production under the IEA Stated Policies moderate scenario was simulated over 2025–2050, producing a temporal profile of active deposits and corresponding production (Fig. 4a), with a total simulated production of 702 Mt compared to 731 Mt of demand, corresponding to the depletion of 30.3% of the studied copper resources. Periods where demand exceeded the supply capacity of available deposits were highlighted in the schedule. Of the 852 porphyry deposits considered, 699 met the minimum mine-life threshold of 10 years and

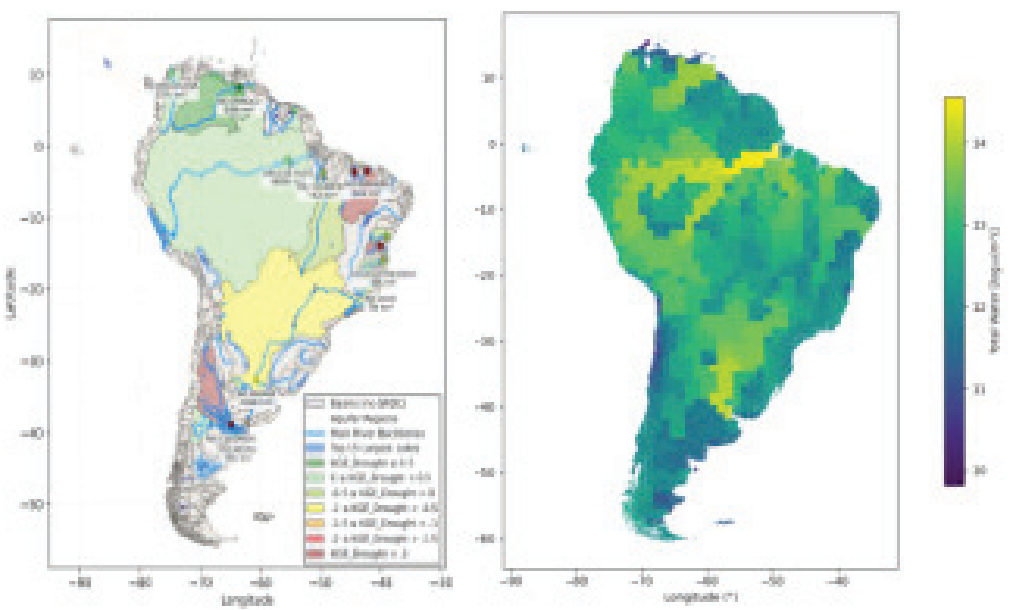

a) Historical validation results *b) Future total extractable water*

Figure 3 *(a) Historical validation of HyIR using the drought-KGE metric in South America, and (b) projected extractable water availability under SSP2-4.5, computed as the sum of lake, river, and aquifer contributions.*

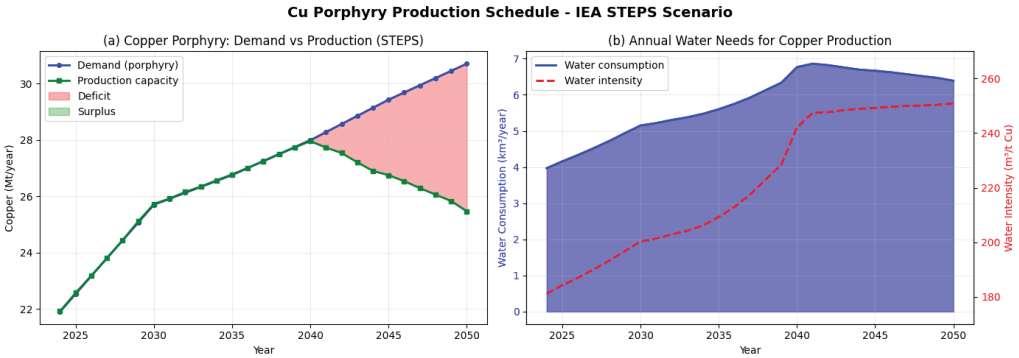

Figure 4 Global production scheduling (a) and associated annual water demand (b).

were therefore included in the production assessment, representing 2318 Mt of contained copper (99.7% of 2326 Mt identified across all deposits). The 153 excluded deposits accounted for 7.9 Mt of copper (0.3% of identified copper). Water requirements for the activated deposits were simulated (Fig. 4b), the deposit-level water intensity had a mean of 365 m^3 t^{-1} of copper and a median of 265 m^3 t^{-1}, with the 10th and 90th percentiles at 123 and 608 m^3 t^{-1} respectively, variability being primarily controlled by differences in ore grade.

Monthly mining water stress was evaluated for 2030, 2040, and 2050 under TaiESM1 SSP2-4.5 forcing and the applied production schedule (Fig. 5). Stress levels exceeding 20% were identified in multiple hydrological grid cells across the assessment period. The stress classification (<10%, 10–20%, 20–40%, 40–80%, >80%) was adapted from the Water Stress Indicator framework (Pfister et al. 2009). However, as only mining water demand was considered, the demand values represented partial withdrawal pressure and therefore underestimated total water stress. In mining-intensive, water-scarce countries such as Australia, Chile, and South Africa, mining accounted for only 2–4.5% of national water withdrawals (Brown, 2003), but local demands could be higher. For this reason, a representative allocation of 10% of gross extractable water was applied to mining, reflecting the coarse spatial resolution and allowing for meaningful assessment of mining-related water stress.

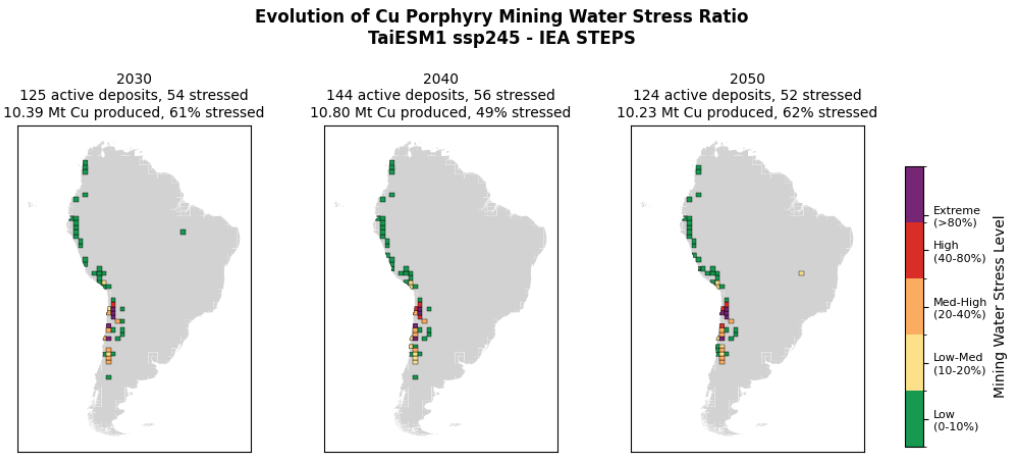

Figure 5 Mining water stress under SSP2-4.5 and STEPS scheduling.

Peak mining-related stress reached 580% in northern Chile in 2034, reflecting the concentration of high-production deposits within a single hydrological grid cell combined with limited local extractable water availability. The same cell exhibited a continuous period above the 20% threshold for 279 months (around 23 years), corresponding to the duration over which deposits in this cell were activated. Thus, highlighting a hotspot where copper production demands reached up to 58% of the total extractable water for all uses in the region. Across South America, the fraction of copper produced from regions exceeding the 20% stress threshold consistently ranged between 49% and 66% of total production throughout the assessment period, indicating that more than half of future copper production in the continent was exposed to medium-to-extreme mining water stress.

Conclusions

Coupling climate projections, hydrological aggregation, and mining production models demonstrated the feasibility of assessing the evolution of water availability for global mineral production. Application of the framework to porphyry copper illustrated its ability to identify spatial and temporal hotspots where production could be constrained by local water resources. Results indicated that a substantial share of future copper production may occur in regions exposed to moderate-to-extreme water stress. Results also indicated the hydrological limitations of grade-based scheduling, highlighting the importance of integrating resource planning with local water availability when evaluating mining operations under changing climatic conditions. Extension of the framework aims to support decision-making by identifying regions where mineral production is most viable under combined production and water availability constraints.

Acknowledgements

The authors thank all co-organisers for hosting the IMWA 2026 Conference.

References

Brown E (2003) Water for a sustainable minerals industry – A review. In Proceedings of the Water in Mining 2003, The Australasian Institute of Mining and Metallurgy

Eyring V, Bony S, Meehl GA, Senior CA, Stevens B, Stouffer RJ, Taylor KE (2016) Overview of the Coupled Model Intercomparison Project Phase 6 (CMIP6) experimental design and organization. *Geoscientific Model Development*, 9(5), 1937–1958. https://doi.org/10.5194/gmd-9-1937-2016

Global Runoff Data Centre (2026) GRDC database. Federal Institute of Hydrology (BfG), Koblenz, Germany. Available at: https://www.bafg.de/GRDC (Accessed 3 March 2026)

Gunson AJ, Klein B, Veiga M, Dunbar S (2012) Reducing mine water requirements. Journal of Cleaner Production 21:71–82. https://doi.org/10.1016/j.jclepro.2011.08.020

International Energy Agency (2024) Global critical minerals outlook 2024. IEA, Paris. Available at: https://www.iea.org/reports/global-critical-minerals-outlook-2024

Knoben WJM, Freer JE, Woods RA (2019) Technical note: Inherent benchmark or not? Comparing Nash–Sutcliffe and Kling–Gupta efficiency scores. Hydrology and Earth System Sciences 23:4323–4331. https://doi.org/10.5194/hess-23-4323-2019

Lakshman S (2024) More critical minerals mining could strain water supplies in stressed regions

Lee W-L, Wang Y-C, Shiu C-J, et al (2020) Taiwan Earth System Model Version 1: description and evaluation of mean state. Geoscientific Model Development 13:3887–3904. https://doi.org/10.5194/gmd-13-3887-2020

Magnin BP, Graham GE, Huston DL, Eglington BM (2025) A global database of porphyry copper deposits and prospects

Northey SA, Mudd GM, Werner TT, et al (2017) The exposure of global base metal resources to water criticality, scarcity and climate change. Global Environmental Change 44:109–124. https://doi.org/10.1016/j.gloenvcha.2017.04.004

Pfister S, Koehler A, Hellweg S (2009) Assessing the environmental impacts of freshwater consumption in LCA. Environmental Science & Technology 43:4098–4104. https://doi.org/10.1021/es802423e

Schaefli B, Gupta H (2007) Do Nash values have value? Hydrological Processes 21:2075–2080. https://doi.org/10.1002/hyp.6825